Urban growth trend analysis of proposed Greater Silchar City, India, using landscape metrics and Shannon entropy model

Divya Prakash Mohabey[1] · Jenita M. Nongkynrih[2] · Upendra Kumar[1]

Abstract

Most cities in the world suffer from excessive population and unplanned urban growth. The objective of the present study was to investigate the spatiotemporal changes of built-up areas and their growth in the proposed Greater Silchar City (GSC) (Assam, India). The obtained LANDSAT satellite data from 1991 to 2021 for the GSC have divided into non-built-up and built-up land use categories, and recode tools in Erdas Imagine 2014 software have been used to improve the accuracy of the output. The study area has been classified into 8 spatial directions and 11 concentric circles with radial distances of 1 km and resulted from intersected areas consisting of 60 gradient zones. The study used Shannon entropy model for detailed urban sprawl study of every nook and corner. FRAGSTATS v4.2 tools have been used to analyse landscape metrics in respective spatial directions. The built-up area growth of the city was 15.18 km^2 during the mentioned period. The landscape metrics and LU/LC results show the maximum built-up growth has taken place in South to South-West direction (3243.87 ha) and the area within a 2–3-km radius (221.85 ha) of the central business district, which is the periphery of the existing Silchar municipal limits. The entropy values indicated that the GSC has compacted infill growth form in the core area, while the dispersed urban sprawl trends followed with increasing distance from the city centre. Moreover, the research findings will provide a conceptual model for assessing urban growth trends for other cities as well.

Keywords Shannon entropy · Landscape metrics · Fragmentation · Urban sprawl and growth

✉ Divya Prakash Mohabey
divyaprakash.mohabey@gmail.com

Jenita M. Nongkynrih
jnongkynrih@gmail.com

Upendra Kumar
upendra_kumar72@rediffmail.com

1   Department of Civil Engineering, National Institute of Technology Silchar, Assam 788010, India

2   Department of Space, North Eastern Space Applications Centre, Government of India, Umiam, Meghalaya 793104, India

1 Introduction

The subject of urbanization has indeed received significant attention over the last few decades due to its substantial impact on economic development and environmental concern in emerging nations. Rapid urbanization is driven by factors such as higher birth rates and large-scale migration from rural to urban areas in search of better employment opportunities and higher living standards (Deribew, 2020). As the population rises, urban areas expand to accommodate the growth, resulting in urban growth beyond their defined limit (Farooq & Muslim, 2014). Urban growth is influenced by various factors, such as available space, geographical conditions, resources, economic and political strength (Mohamed, 2017). Urbanization is the best example of irreversible land conversion from agricultural and productive land to urban areas, which impacts the local environment, natural resources and the surroundings of urban areas (Altieri et al., 2019; Reddy, 2017). The evolution of population and infrastructure within a city in a positive manner is referred to as urban growth. In contrast, urban sprawl refers to the uncontrolled and unplanned urban growth within the city, surrounding and rural areas, characterized by low-density housing and businesses, which leads to unsustainable urbanization (Anees et al., 2019; Liu et al., 2020; Pourghasemi et al., 2012). However, most cities worldwide are experiencing inconsistency in their expansion, which leads to urban sprawl (V. P. Mandal et al., 2014; Mohamed, 2017). There are some common types of urban growth and sprawl patterns, such as vacant or unused land that may transform into high-density urban growth through infill (inside the city's boundaries), linear (city enlargement through time near roadways), cluster (new group formation) and scattered expansion (new built-up expansion activity on the periphery in a short period) (Mohabey et al., 2023; Weerakoon, 2017). Urban sprawl has serious consequences, including environmental degradation, ecological destruction, cropland and vegetation cover loss, deforestation and air and water contamination (Akhter & Noon, 2016; Mohammady & Delavar, 2016). In fact, unplanned growth gives rise to issues such as traffic, overcrowds, climatic scenarios, increased runoff, urban flooding and waterlogging (Ilyassova et al., 2021; Noor et al., 2014; Saini et al., 2019).

Traditional mapping and surveying techniques were time-consuming and uneconomical for urban growth study. Therefore, to effectively monitor, analyse and map land use and urban development trends, researchers have suggested the utilization of remote sensing (RS), geographical information system (GIS) techniques and statistical methods. These advanced tools and methodologies have the capability to provide highly effective results in understanding the dynamics of land use changes and urban growth (Kumar et al., 2020; Toosi et al., 2022). There are several GIS methods available for urban assessments, i.e. cellular automata (CA) models (Anees et al., 2019; Harig et al., 2021; Ilyassova et al., 2021); Entropy models (Altieri et al., 2019; Chatterjee et al., 2016; Deribew, 2020; Mohabey et al., 2023), landscape metrics models, etc., (Dhanaraj & Angadi, 2022; Kowe et al., 2015). However, the Shannon entropy model and landscape fragmentation metrics are the most suitable methods for evaluating urban sprawl and growth pattern (Cegielska et al., 2018; Vani & Prasad, 2020). Shannon entropy is an emerging mathematical communication theory that has also been used in various fields over the past five decades for analysing the degree of spatiotemporal exposure and urban built-up land distribution (Dhali et al., 2019). In Shannon entropy model, the built-up pixel values of satellite data, which are proportional to their relevant information, are used to estimate the sprawl pattern of any urban area (Dhanaraj & Angadi, 2020; Mohabey et al., 2023). The advantages of Shannon

entropy are to reveal the degree of instability, unbalance and uncertainty of urban sprawl by assessing whether urban growth is scattered or compact (by numerical values) (Mithun et al., 2021; Patra et al., 2022; Yulianto et al., 2020). Like other countries, most of the cities in India are experiencing exponential growth in built-up areas and population density, leading to urban sprawl (Bhat et al., 2017; Chettry & Surawar, 2020). Numerous studies have been conducted worldwide; however, specific studies focusing on monitoring urban growth using Shannon entropy model in the Indian context are highlighted here. Punia and Singh, (2012) used Shannon entropy approach to estimate the urban growth of Jaipur City, Rajasthan (1975–2006), at ward and city levels which resulted in a 78% variation of urban built-up land. The city has initially scattered structure which further developed into a dense form in the core area, while new built-up continued to expand in the peripheral area. Dhali et al., (2019) conducted a study to monitor the spatiotemporal urban growth of various sub-centre of the North 24 Parganas district, West Bengal (1989–2016). Most of the urban sprawl is a result of transforming barren and agricultural land into built-up areas. Pawe and Saikia, (2020) observed an uneven intensity of built-up growth in the Guwahati Metropolitan (1976 to 2015), resulting in if current trends continue, future urban sprawl may lead to weak sustainability and threaten the ecosystem and semi-urban areas. Patra et al., (2022) have used the relative Shannon entropy model and gradient area classification approach for urban sprawl analysis of Cuttack City, Odisha, from 1990 to 2018. They suggested that the entropy analysis method is easy and reliable for urban growth pattern analysis. The built-up area of the city has increased by 46.75% during the mentioned period.

An urban system consisting of complex landscape elements characterized by diverse land uses as a result of various interactions between the community and nature (Yang et al., 2021). Urban landscapes generally consist of different elements arranged in different spatial configurations. These patterns were formed by a complex interplay of many factors over many years (Chettry & Surawar, 2021; Shifaw et al., 2020). Urban spatial patterns can be quantified using landscape metrics to understand urban development trends and functions (Mithun et al., 2021). The landscape indices comprise identifying patterns in landscapes, geomorphology, ecological fragmentation, assessments of landscape variations and exploration of the impacts on the landscape structures (Feng & Li, 2012; Jaafari et al., 2016). Landscape metrics have gained popularity in the field of ecology earlier and later in monitoring urban growth (Tian & Chen, 2021; Toosi et al., 2022). It is an excellent approach to measuring spatial form and urban sprawl (McGarigal & Marks, 1995). In addition to landscape metrics, the gradient and zone analysis approach plays an important role in determining the spatial pattern to identify the type of urbanization, and FRAGSTATS software offers the widest choice of landscape metrics and is built to be as versatile and efficient as possible (Chatterjee et al., 2016; Das & Angadi, 2021; Dhanaraj & Angadi, 2020, 2022; S. Mandal et al., 2020). Several researchers have used landscape fragmentation analysis methods to study urban growth in Indian cities. Anees et al., (2019) studied Kurukshetra City by landscape metrics method, resulting in land fragmentation with a mix of development patterns over the past decades, and urban core density has been associated with increasing land fragmentation. Without proper management and regulations, the city may turn into a mega city, and the urban sprawl on the agricultural land and the city's periphery may cause serious environmental imbalance. S. Mandal et al., (2020) have used a gradient area classification approach for landscape fragmentation to monitor and measure urban forms of Howrah City's spatial metrics (1996–2016). They observed that the combination of the techniques, as mentioned earlier, provides specific information on periodic changes in urban growth types. Chettry and Surawar, (2021) conducted a combined

study for urban sprawl analysis for eight mid-size Indian cities of Lucknow, Patna, Ranchi, Raipur, Thiruvananthapuram, Bhubaneswar, Srinagar and Dehradun from 1991 to 2018, and resulting the modern landscape research tools depicting the scientific evidence of urban sprawl.

At the same time, several researchers have used both (Shannon entropy and landscape fragmentation metrics) approaches to study urban growth and sprawl in Indian cities. Jat et al., (2008) conducted a study for modelling the urban growth of Ajmer City (1977–2005), which revealed a 200% urban sprawl on spatial distribution using Shannon entropy model and landscape metrics. Chatterjee et al., (2016) used the Shannon entropy index and landscape metrics for modelling urban sprawl around Greater Bhubaneswar City in Odisha (1972 and 2014). Their findings suggest that there was a trend of urban sprawl in the urban area, moving from the city centre to the periphery areas and expanding rapidly in a non-contagious manner. Apart from the main area, most of the residential areas were scattered randomly surrounding the city centre. Thakur et al., (2020) monitored and modelled the urban sprawl (1991–2011) of Shimla city, accounting for 98% variation in urban sprawl with contributing factors. Mithun et al., (2021) studied urban sprawl of Kolkata metropolitan (1996 to 2016) and found that non-urban areas tend to urbanize faster. The results for landscape metrics were mostly independent, and zoning techniques were found to be strong in urban tools for checking built-up transformation. Rath et al., (2022) used Shannon entropy approach and landscape metrics for urban agglomeration (2005 to 2015) study for eastern and southern Indian cities of Bhubaneswar, Cuttack, Chennai, Bengaluru, Hyderabad, Ranchi, Kolkata, Visakhapatnam and Coimbatore. The results show that all cities were grown as compacted by infill growth in the core area and sprawling continuously in the outer fringes. Dhanaraj and Angadi, (2020, 2022) have used Shannon entropy and landscape metrics model to monitor the spatial urban growth in Mangaluru City (1972–2018). The entropy value suggested that every urban growth is compacted by growth around urban centres and is intensively urbanized. Also, growth during the period has led to the creation of many smaller urban centres around the city, indicating the upcoming metropolis transformation. Changes in built-up landscape indices may be indirectly linked to the different socioeconomic and geomorphological conditions of built settlements in the region.

Silchar is one of the most important cities in North-East India and the second-largest city in the state of Assam. Silchar City has witnessed massive population and urban built-up area growth in the last 30 years (1991–2021). The city is congested due to land scarcity and centralized business areas around the city centre (Mohabey et al., 2023). Due to the low price and availability of agricultural and vacant land in the nearby areas, there has been rapid built-up growth in the outskirts of Silchar City. The people from outside and inside of the city always depend on the Silchar urban area to fulfil their needs, such as commercial, official, institutional and medical, which creates the problem of traffic congestion on most roads and also leads to overcrowding of the city. The municipal development authority is responsible for providing basic amenities such as transportation, sanitation, electricity and water supply, educational and medical facilities for people residing on the outskirts of the city. So periodic urban growth evaluation becomes essential for planning and management. Mohabey et al., (2023) carried out a study for the analysis of land use land cover change and urban growth of Silchar City from 2005 to 2018, which covers only 28 wards (total geographical of 15.75 km^2) of the existing municipal limits of the city with the help of Shannon entropy model. This study showed that compact growth is happening

in the core area of the city as well as the outer area is sprawling rapidly. To maintain systematic urban planning and development of current and future aspects, the office of the "Directorate of Town and Country Planning Assam, Government of Assam" has proposed a plan (in the year 2016) to extend the city's municipal boundary, namely the "Greater Silchar City" (GSC). The GSC covers around 112 km^2 area, including the area under Silchar Municipal Corporation (SMC) and its surrounding urban and rural areas. GSC is considered a medium-sized city and has observed the same uncontrolled urban and population growth trends as most Indian cities.

However, no study has been done for the GSC for urban growth trend analysis using any existing methods. The present study is a first-time approach for the area's urban growth and sprawl trend analysis under GSC. The objective of the present study is the delineation of urban growth and sprawl pattern of GSC from 1991 to 2021 using landscape metrics fragmentation tools and Shannon entropy model, respectively. The zonal, concentric circles and gradient approaches have been used as tools to measure urban growth patterns by dividing the GSC area in the spatial distribution system from the city centre. The spatial direction, concentric circle and zonal gradient approach techniques are three distinct spatial approaches followed by the area covered in a particular direction and distance from CBD (centre of the circles and directions). Importantly, these approaches have been applied for the first time in the GSC to understand the urban growth and sprawl phenomena. The main advantage of this research is the addition of new approaches that planners and decision-makers can utilize to obtain a reliable estimate of urban growth, considering various factors such as geography, time and socioeconomic aspects.

2 Study area

The existing Silchar City is the administrative headquarter of the Cachar District, located in the South-Eastern part of the Assam state. The proposed GSC plan boundary covers the area between 92°43′14.058″E to 92°51′52.122″E longitude and 24°43′42.826″N to 24°52′12.801″N latitude with variation in altitude from 17 to 28 m above mean sea level. The GSC covers around 112 km^2 of the total geographical area, whereas 13.64 km^2 of land comes under the existing Silchar Municipal Corporation (SMC), 13.01 km^2 of the urban area outside the periphery of SMC and the 77.27 km^2 of the rural area in the surrounding, while the River Barak covered 7.92 km^2 of land. Premtala Square has been accepted as GSC's Central Business District (CBD) point. It is the central core area of economic and commercial activities. Several shopping malls, daily markets and government civil hospitals are within 1 to 2 km. The details of the study area are shown in Fig. 1. Moderate climate prevails here, with temperatures typically ranging from 7 to 38 °C throughout the year. The annual rainfall in the Silchar region is around 300 cm, and during the monsoon season, it frequently faces floods from the Barak River (the second-largest river in North-East India) (Saha et al., 2022). Other regional natural disasters, such as earthquakes, floods and river bank erosion, continue adversely affecting local people and economic and social activities (Nath & Ghosh, 2022). Tea, rice, vegetables, crops and herbs are mainly cultivated. The GSC region is well connected by railways, highways and road networks, including airports, which connect to Mizoram, Manipur, Tripura, Meghalaya states and Guwahati City (Ashwini & Sil, 2019).
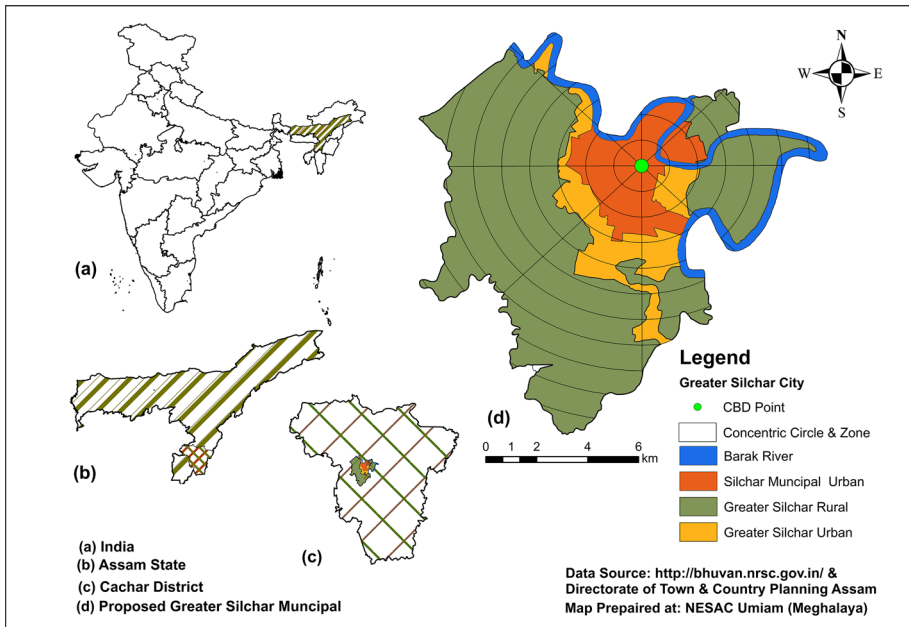
Fig. 1 Maps of the study area: **a** India, **b** Assam State, **c** Cachar District and **d** Greater Silchar City

3 Materials and methods

3.1 Materials

Land use/land cover (LU/LC) data are the primary need for most of the analysis, including urban growth, changes and sprawl pattern studies (Mohabey & Kumar, 2015). To classify LU/LC changes and compute urban sprawl in the GSC, multi-spatial and temporal open-source LANDSAT 5-TM, 7-ETM and 8-OLI TIRS satellite images (multi-spectral resolution of 30 m) from the years 1991, 2001, 2011 and 2021 were obtained from the "United States Geological Survey (USGS)" website (Mithun et al., 2021). This region comes under the UTM-Zone 46 N Projection and WGS-84 datum; LANDSAT images follow the Path: 136/Row: 43. All satellite data used for the LU/LC have been taken in the month of February as the region remains cloud-free. Moreover, during this month, the waterlogged area gets dried; hence, the grassland, agricultural land, tree cover and built-up settlements can be easily identified. The collected LANDSAT satellite images sometimes need pre-processing such as geo-referencing, ortho-rectification, image enhancement and atmospheric corrections (Jain et al., 2011; Sharma et al., 2020), which have been rectified with the help of ArcGis10.6 and Erdas Imagin 14. Figure 2 shows a schematic representation of the methodology for built-up growth analysis of the GSC.

The map boundary of Silchar City has been acquired from North Eastern Space Applications Centre (NESAC), Umiam, Meghalaya, India. At the same time, the GSC development plan.pdf file format map was obtained from the "Directorate of Town and Country Planning Assam, India." Then the boundary is generated as a shape file (.shp) in vector format by the geo-referencing and digitization techniques. This shape file includes the data
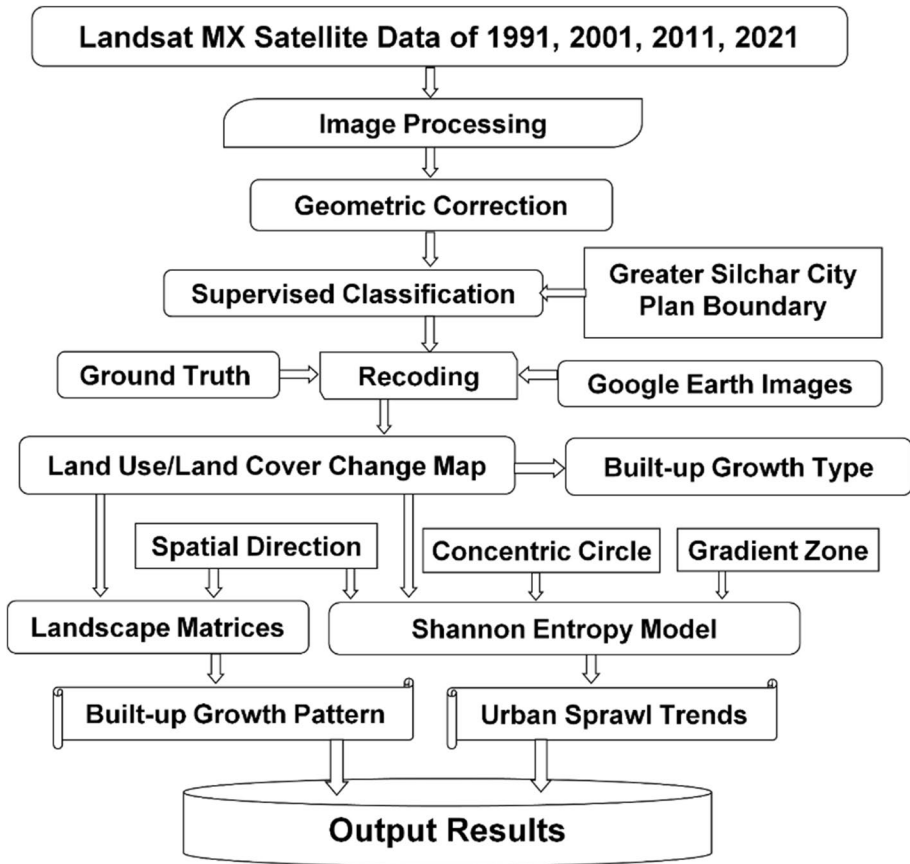
Fig. 2 Flow diagram of the methodology

of existing wards under Silchar Municipal Corporation (SMC) and the wards which comes under the urban category to the outside of the SMC boundary and surrounding rural areas (villages) in the GSC. The field survey was conducted (in 2021) with the help of GPS enabled camera and smartphone for doubtful areas and accuracy assessments.

3.2 Urban land use extraction

The supervised classification technique has been found suitable for delineating land use classes. The nearest neighbourhood and maximum likelihood classification (MLC) approaches have been used for the LU/LC analysis with the help of Erdas Imagine 2014 software (Shikary & Rudra, 2021). LU/LC has been classified into two classes: built-up settlements, and the remaining are integrated into non-built-up class (Singh & Sarkar, 2020). The multi-temporal and quantitative analyses have been used to quantify, map and evaluate urban growth patterns based on the built-up area analysis. Built-up areas comprise urban or built-up lands, including industrial, commercial, residential, communications, transportation, services and utility regions. The non-built-up land contains agricultural fields, open spaces, water bodies, tree cover, etc. (Reddy, 2017).

In multi-temporal images, several inconsistencies and errors were observed due to vignetting effects in the pictures, seasonal changes in sunlight conditions and radiometric distortions between different dates of aerial photograph capture, etc. (Altieri et al., 2019). When using medium-resolution (LANDSAT data) satellite images, increased tree cover obscures the built-up area, allowing pixels to produce inaccurate results with few errors. It has been overcome by using a recording process through visual interpretation with Google Earth and field survey data. The recode tool in the ERDAS IMAGINE 2014 software has been used for better accuracy of output results than the previous ones (Dhanaraj & Angadi, 2021; Thakur et al., 2020). These classified data have been used for further assessment of urban growth by the landscape metrics and Shannon entropy approach (Anees et al., 2019).

3.3 Types of urban growth patterns

The urban built-up growth in the GSC area follows various patterns, as described further. The infill growth occurs under city limits where open space or vacant land may convert into built-up land. The positive aspect of this kind of growth is that the municipal body can easily handle and create plans to provide necessary facilities, leading to compact urban areas (Akhter & Noon, 2016). The linear or ribbon growth describes rows of built-up growth beside existing highways (river banks, railways or other similar linear structures), each accessed by a dedicated entrance. Leapfrog growth is a dispersed type of urbanization with irregular urban land use expansions (Harig et al., 2021). Leapfrog growth occurs when people construct residential or other built-up far from an established city, bypassing the vacant lands closer to the municipality. Scattered or dispersed growth may refer to the random and unsystematic built-up growth in large open areas without following development rules (Dhanaraj & Angadi, 2022; Noor et al., 2014). Figure 3 represents the built-up growth pattern.
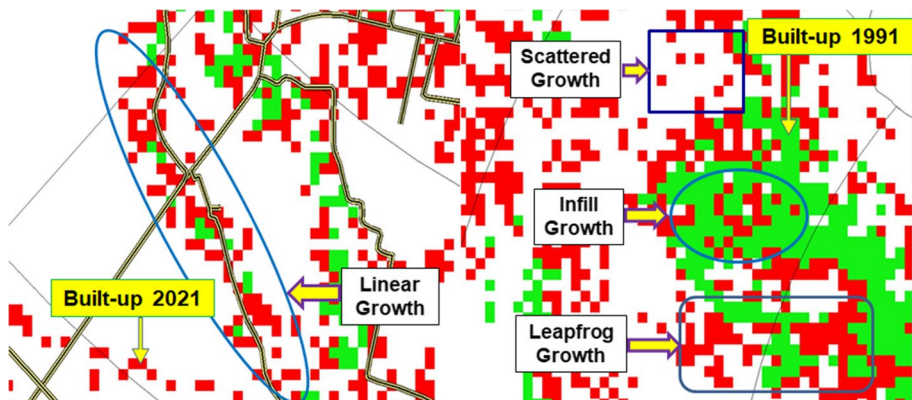

Fig. 3 Types of built-up growth patterns

3.4 Built-up area analysis approaches

3.4.1 Spatial directional approach

Based on the patch pattern produced in the research area for the years 1991, 2001, 2011 and 2021, the study region was divided into eight regions (Fig. 4): North (N), North-East (NE), East (E), South-East (SE), South (S), South-West (SW), West (W) and North-West (NW) (Chettry & Surawar, 2021) to account for the unevenness of urban expansion in spatial directions from the city's CBD (Rastogi & Jain, 2018; Shikary & Rudra, 2021).

3.4.2 Concentric circles approach

This concept is based on the Burgess hypothesis, which was developed in 1924 and asserts that cities expand in a circular pattern from the centre to the outward (Burgess, 2015). As a result, the circle is the only geometric form that can meet the criteria of equal distances in all directions, making it the perfect shape to help us understand how cities evolve. To comprehend the structure of the urban built-up area, a circular region of 11 km (maximum) from the city centre (CBD) is divided into concentric circles (rings) with an incrementing radius of 1 km using the gradient analysis technique (Fig. 5). This illustration shows how land use varies in every kilometre (Mishra et al., 2011).
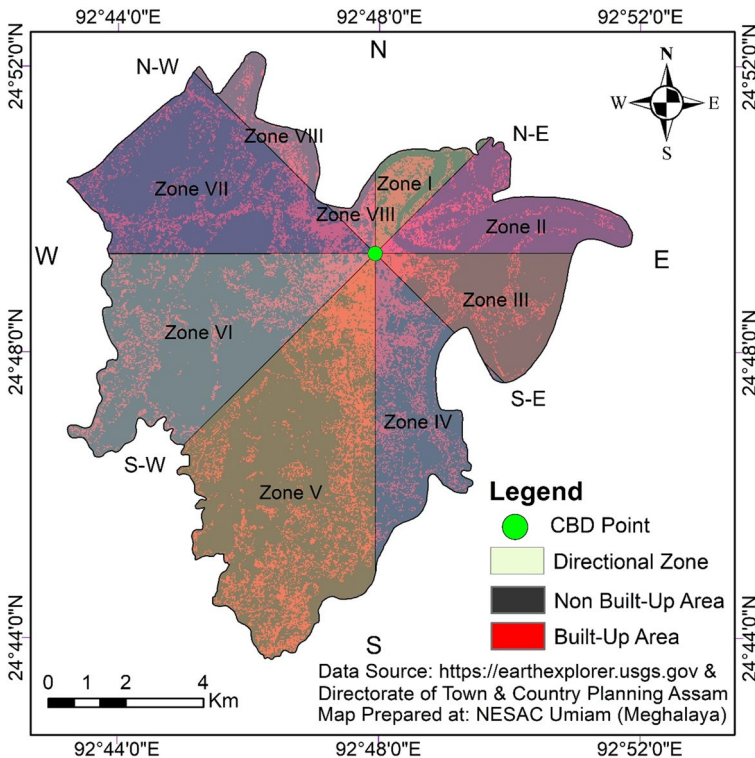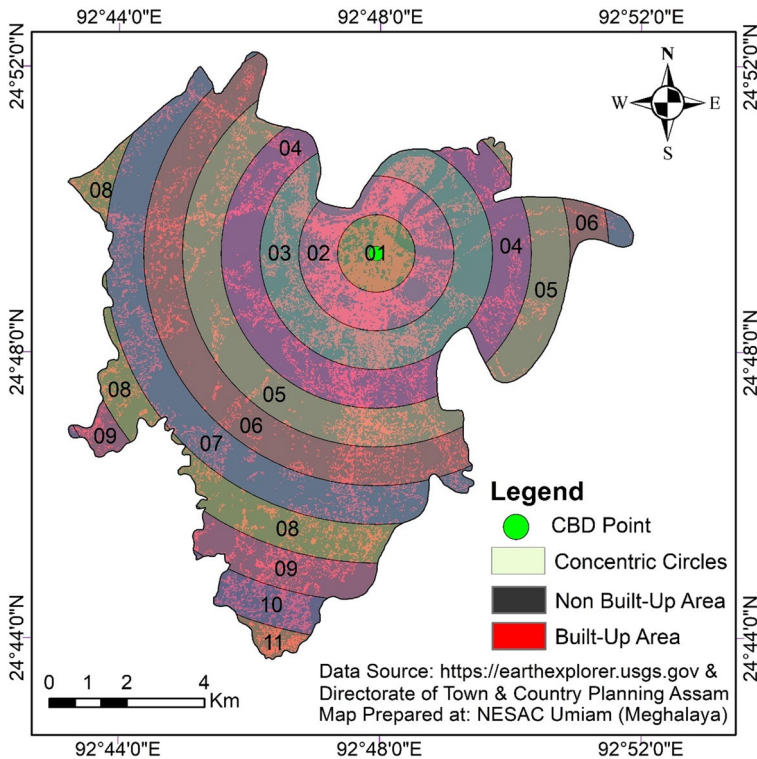

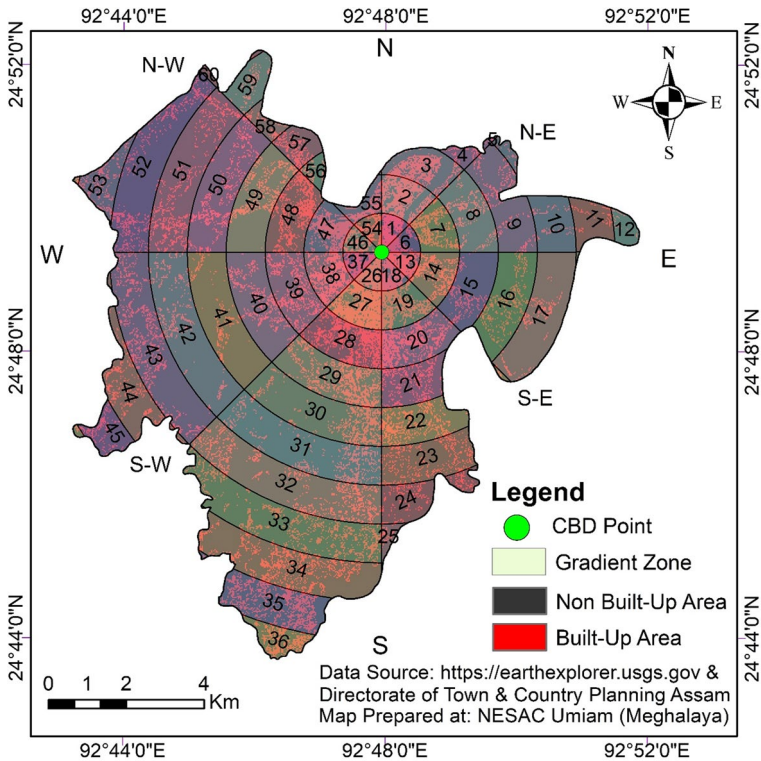**Fig. 4** Map of divisions of the study area into the spatial direction

Fig. 5 Map of the division of the study area into concentric circle approach of the incrementing radius of 1 km

3.4.3 Gradient zonal approach

To trace urban growth at every nook and corner for the better understanding of the processes of profound transformations of the GSC, the integrated spatial zone and the concentric circle (ring) are allocated into gradient zones (GZ) from the centre (CBD) to the outskirts (Chatterjee et al., 2016), as considered the third approach. The study area has been covered under 60 gradient zones (GZs) (Fig. 6).

3.5 Urban landscape pattern metrics

Landscape metrics have been widely used for built-up growth analysis (Shukla & Jain, 2019; Tian & Chen, 2021). Metrics to measure landscape patterns define and quantify spatial variability's size, origin and effects in different landscape patches (Frazier & Kedron, 2017; Jaafari et al., 2016). These indices show the spatial organization of the urban patch, the interaction between the patch and the surrounding landscape and changes in the landscape over the time (Azhdari et al., 2018). Various elements are generally arranged in diverse ways throughout the urban landscape. These measures are used to track changes in the land surface. At the same time, these techniques have the

Fig. 6 Map of the division of the study area into the gradient zone approach

potential to identify the causes, effects and current as well as future trends of urban growth patterns (Mohabey et al., 2015). For estimating the spatial pattern index values in the present study, we utilized the urban built-up patches from the LU/LC data of the study area (Malarvizhi et al., 2022; Toosi et al., 2022). Landscape patch metrics are used to investigate various urban patch features to gain a deeper understanding of the dynamics of urban expansion, its origins and subsequent consequences (Jahani & Barghjelveh, 2021; Nagendra et al., 2004; Shukla & Jain, 2019). The spatial zonal approach has been used to assess urban built-up growth landscape indices. To characterize landscape patches, Fragstats provides a variety of landscape metrics. Spatial indices were calculated using FRAGSTATS v4.2, with the generated images in GeoTiff grid (.tif) format as input data and a file as a comma-delimited ASCII file to provide information on each intake scenario.

3.6 Quantifying change in landscape configuration

Area edge metrics relate to the recipient of measurement, size, shape and area of the patch edge (Dhanaraj & Angadi, 2022). This method of data collection has thus made it simpler to understand trends in urban expansion in GSC. The most important landscape indices for urban growth analysis are as follows.

3.6.1 Landscape metrics

Calculations are algorithmic tools that measure specific spatial behaviour of different patches, groups of individual patches or complete mosaics of a landscape. Numerous landscape metrics have been established to characterize landscape structures and geographical variability based on landscape patterns and layouts (Frazier & Kedron, 2017; Shifaw et al., 2020).

- *Class Area (CA)* is a fundamental metric used to represent the trend of urban expansion in spatial metrics estimation, also defined as the total area, suggesting the entire area is covered by a particular LU/LC class in hectares. This reflects how much of the landscape is made up of a specific patch type. Aside from its direct, it represents the overall class area in m^2 as of all relevant patches divided by 10,000 (to convert to hectares) and ranges between CA > 0 and no limit (Das et al., 2021; Jain et al., 2011).

$$CA = \sum_{n=1}^{x} \alpha_{mn} \left(\frac{1}{10000} \right) \tag{1}$$

    Variables: α_{mn} = patch area and n = x number of patches.
- *Edge density (ED)* is directly connected with changes in the intensity of disturbance across small ranges, with the gradient of the connection being influenced by patch size and irregularity. A rise in urban edges can be easily measured using edge density. The ratio of the built-up patches to the edge of patches and the surroundings significantly affects this measurement. Small patches will have greater edge density than landscapes with large patches. It is the sum of the lengths (m) of all edge segments involving the corresponding patch type, divided by the total landscape area (m^2), multiplied by 10,000 (to convert to hectares) (Das et al., 2021; S. Mandal et al., 2020; Narmada et al., 2021).

$$ED = \frac{\sum_{l=1}^{x} E_{il}}{\beta} * 10000 \tag{2}$$

    Variables: β = total area landscape and E_{il} = the number of edges.
    The range is without limit in ED ≥ 0.
- *Total edge (TE)* is a method to quantify the fragmentation of LU/LC. It is an exact measurement of the overall length of all edges in a specific patch type or across all types of patches (Kowe et al., 2015). Large TE values suggest continuous, extensive urban regions. An increase in total edge indicates more area fragmentation.

$$TE = E \tag{3}$$

    It is measured in metres, and the range always has no limit to TE ≥ 0.

3.6.2 Subdivision metrics

The subdivision indices intend to measure how fragmentary the landscape is regarding patch shape, location and arrangements. These metrics are related to the aggregation index and measure disaggregation (Jain et al., 2011; Kowe et al., 2015; Yang et al., 2021).

- *Number of Patches (NP)* metric is used to quantify patch fragmentation within each LU/LC class. The total number of patches of the same type is known as NP. It measures irregularly shaped urban areas or independent landscape features. This allows for rapid core expansion and the formation of additional fragmented patches around the core, resulting in increased patches. The amount of this patch reflects the richness or complexity of the landscape (Anees et al., 2019; Jain et al., 2011; Kowe et al., 2015).

$$NP = n_i \tag{4}$$

    Variable: n = number of patches.
    Its range is always NP ≥ 1, with no limit and no units.

- *Patch Density (PD)* of the dispersed urban structures inside a given region is specified by this additional measure of landscape fragmentation of a LU/LC class. Since it is a key factor in characterizing individual patches, the levels of this element are influenced by the minimum mapping unit as well as pixel size (Anees et al., 2019; Jahani & Barghjelveh, 2021; McGarigal & Marks, 1995). PD typically represents the number of patches as an area function, allowing for various sizes comparisons of landscapes.

$$PD = \frac{N}{\beta} \tag{5}$$

    Variables: N = number of total patches and β = total landscape area.
    The range is without limit in PD ≥ 0, and unit in metre square (multiplied by 10,000 to convert hectares)

- *Largest Patch Index (LPI)* determines the segments of the largest patch that contribute to the overall area of the landscape, revealing the existing growth of the urban centre. It is calculated by multiplying the ratio of the area of the largest patches to the respective patch type by 100 (to turn it into percentages) (S. Mandal et al., 2020; Narmada et al., 2021).

$$\text{LPI} = \frac{\max_{m=1}^{x} \left(\alpha_{\text{mn}} \right)}{\beta} * (100) \tag{6}$$

    Variables: α_{mn} = patch area and β = total area of landscape.
    Its values output on percentages and range is always 0 < LPI ≤ 100.

3.6.3 Aggregation metrics

Aggregation metrics are assessments of how many patches are in a landscape and their scatter and interspersion. By using the Landscape Shape Index (LSI), one can identify the irregularities in patch shapes, as the LSI increases with the new centre of urban areas and decreases with older ones(Jaafari et al., 2016; Jahani & Barghjelveh, 2021).

- *Landscape Shape Index (LSI)* is simply the sum of the landscape limit (whether it represents a true edge or false) and all edge sections (m) inside the landscape limit (including such borderline in the background) to the square root of the entire landscape region (m^2), corrected by a steady for a radial standard (vector) or square level (raster) (Anees et al., 2019; Kowe et al., 2015).

$$LSI = \frac{0.25E'}{\sqrt{\beta}} \tag{7}$$

Variables: β = total area landscape and E' = number of edges
Its range is always LSI $\geq$ 1, with no limit and no units.

3.6.4 Shape metrics

At the patches, class and landscape factors, Fragstats calculates several statistics that measure landscape components by the specific patch form. The relationship between patch form and size can influence numerous significant LU/LC processes.

- *Area-Weighted Mean Patch Fractal Dimension (AWMPFD or FRAC_MN)*. The average size of LU/LC patches in a specific area or along the overall landscape is known as the "Mean Patch Size" (AREA_MN). It is a way of measuring the subdivision of LU/LC class or landscape. The AWMPFD equations are adjusted to account for the interference in the patches perimeter by containing two times the logarithm of patch perimeter (m) divided by the logarithm of patch area (m^2), then multiplied by that of the patch area and divided by the overall landscape. AWMPFD stands for the patch fractal dimension (FRACT) average of patches within the landscape area, balanced by patch area (Kowe et al., 2015; S. Mandal et al., 2020; Yang et al., 2021).

$$FRAC\_AM = \sum_{m=1}^{x} \sum_{n=i}^{y} \left[\left(\frac{2\ln(0.25\rho_{mn})}{\ln x} \right) \left(\frac{\alpha_{mn}}{\beta} \right) \right] \tag{8}$$

Variable: α_{mn} = patch area, x = number of patches, ρ_{mn} = patch perimeter and β = total area landscape.

3.7 Shannon entropy approach

With the use of GIS and remote sensing, entropy can be considered the most valuable means to investigate the extent of urban growth and sprawl. This model reflects the regional concentration or dispersion of a certain LU/LC class, making it a better choice for comparing two or more phases of urban growth. The Shannon entropy estimates the average unpredictability of a random variable, which is proportional to its relevant information (Du et al., 2022; Malarvizhi et al., 2022). Entropy values range from 0 to log(n) and measure how much built-up land is expanding and sprawling in an urban built-up region (Patra et al., 2022; Punia & Singh, 2012). Entropy can be near to 0 when a value is highly concentrated, whereas entropy close to log(n) suggests a highly dispersed value (Horo & Punia, 2019; Mithun et al., 2021; Shukla & Jain, 2019). Most urban areas have densely populated areas in their centres and sprawled outward.

The entropy (H_n) of the urban built-up settlements can be calculated using the following equation,

$$H_n = \sum_{m=1}^{n} \rho_m * \log\left(\frac{1}{\rho_m} \right) \tag{9}$$

where ρ_m shows the variable quantity in the mth zone and n is the total number of zones or concentric circles.

$$\rho_m = \frac{x_m}{\sum_{m=1}^{n} x_m} \tag{10}$$

where x_m is the observed urban patches in the respective zone.

For the present study, the Shannon entropy of the urban built-up patches has been analysed in all three spatial zonal approaches with respect to CBD. The entropy values for each portion of the GSC have been obtained by computing the entropy from the land use built-up data. This approach is trustworthy since it can identify growth and sprawl patterns in any urban area.

4 Results and discussion

4.1 Urban built-up landscape fragmentation analysis based on a spatial direction approach

- *Class Area (CA)*—The maximum built-up class area in the S-SW direction (Fig. 7(a)) has doubled in the last three decades, from 266.58 in 1991 to 824.22 ha in 2021. Zone-VIII and zone II found a minimum built-up class area expansion.
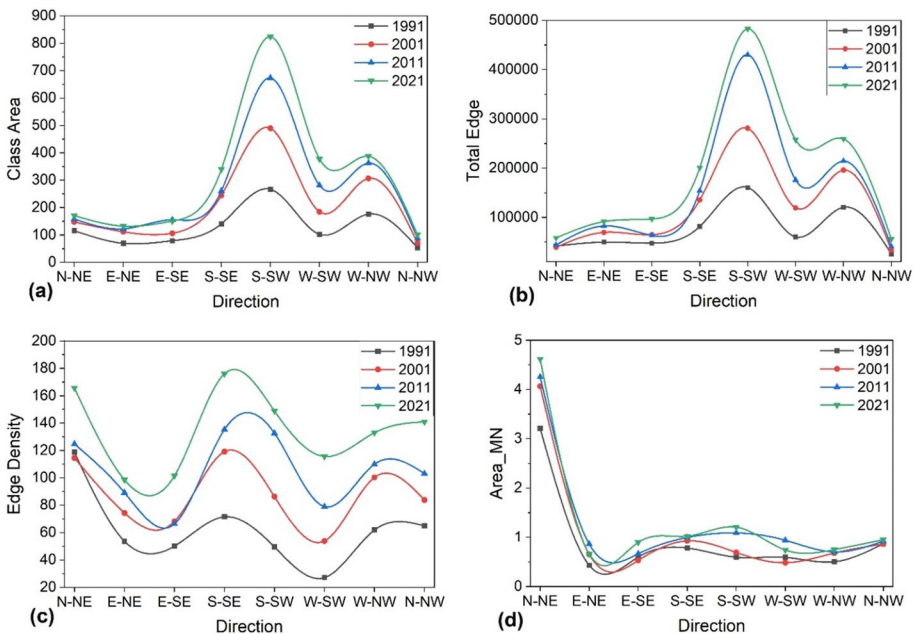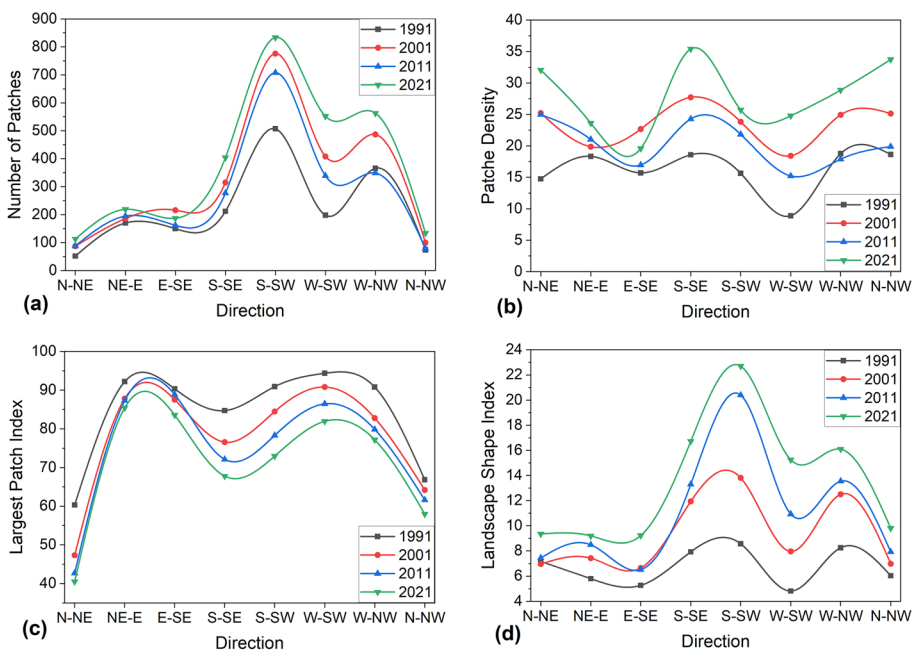

Fig. 7 Different class-edge metrics of built-up patches CDB for spatial directions during 1991–2021 **a** class area, **b** total edge, **c** edge density and **d** Area_MN

- *Edge density (ED)*—The maximum increment in edge density is found in W-SW and S-SW from 1991 to 2021, which means the urban area growth rate in this direction is higher than in other zones (Fig. 7(b)).
- *Total edge (TE)*—The urban areas were discontinuous growth from 1991 to 2021 because edges were narrower, and the landscape was more dispersed (Fig. 7(c)). The TE data indicates that edges constantly developed from 1991 to 2021, and S-SW and S-SE directions significantly increased.
- *Mean patch size (Area_MN)*—Metrics generated from patch areas offer opposing perspectives on patch size as well as on the fragmentation of the landscape. Zone I (N-NE) (Fig. 7(d)) covers the minimum geographical land of the study area but is densely populated and near to CBD, giving maximum AREA_MN values. Zone V (S-SW) has covered the maximum geographical land, and the values of AREA_MN have found a high growth rate compared to other zones.

4.2 Subdivision patch metrics

- *The Number of Urban Patches (NP)*—It measures how fragmented built-up regions are. Figure 8(a) represents the number of settlement built-up patches by directional zone over various periods. In almost every zone, there was a significant rise in NP from 1991 to 2021, indicating that the landscape grew progressively fragmented after 1991. The NP values were reduced in the N-NE and N-NW; this reduction explains how the patches aggregated. The directions S-E, NW-W and S-SW had a considerable rise. In most cases, built-up patches significantly increased, especially at the margins of the

Fig. 8 Different area-edge metrics of built-up patches CDB for spatial directions during 1991–2021: **a** number of patches, **b** patch density, **c** LPI and **d** LSI

NW direction. Therefore, it suggests that urban expansion will occur continuously in all directions.

- *Patch Density (PD)*—It exhibits a higher rising tendency in PD values towards the N-NE, N-NW and S-SW directions having a higher rate of expansion showing spatial discontinuity of built-up patches (Fig. 8b). In contrast, lower growth rates have been found in zones III and IV; the patch density increased around four times in the W-SW directions and has lower values near the city centre.
- *Largest Patch Index (LPI)*—The zone II LPI metric was much greater than zone V and zone III, and zone VI LPI is the largest among them (Fig. 8c). It represents the percentage of land patches decreasing from 1991 to 2021. The lower LPI was detected in zone I in 2021, indicating a decreasing trend in LPI, meaning the built-up land has grown and tends to rise on compactness.
- *Landscape Shape Index (LSI)*—The LSI is a simple approach to identifying the aggregation and dispersion of urban patches. Figure 8d illustrates the minimal LSI values in the W-SW and E-SE directions in1991, showing simpler forms and more compact settlement areas. Between 1991 and 2021, the N-NE direction indicates minimal changes, whereas the S-SW direction reveals significant increases in LSI values.

4.3 Shape metrics

Area-Weighted Mean Patch Fractal Dimension (AWMPFD or FRAC_MN) is a shape metrics, the average patches inside the landscape area balanced by the patch area. Herein, the years 1991 and 2011 indicate higher fluctuating trends (Fig. 9). S-SE and N-NW directions show FRACT_MN values close, while W-SW and W-NW directions values was far from central values.

4.4 Urban built-up growth and Shannon entropy index

All three area classification approaches have been used for the Shannon entropy exploration of the study from 1991 to 2021. Figure 10 represents the urban built-up growth of the GSC. Tables 1 and 2 represent the details of spatial direction-wise and concentric circle-wise built-up area, changes and Shannon entropy values, respectively. Figures 11 and 12 are the graphical and map representation of gradient zone-wise Shannon entropy values

Fig. 9 Shape metrics (FRAC_MN) of built-up patches CDB for different directions from 1991 to 2021
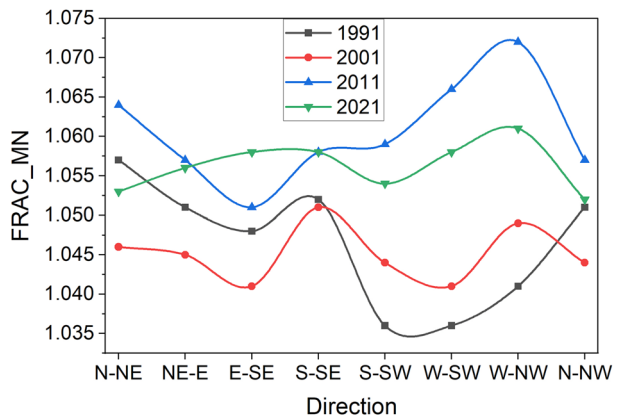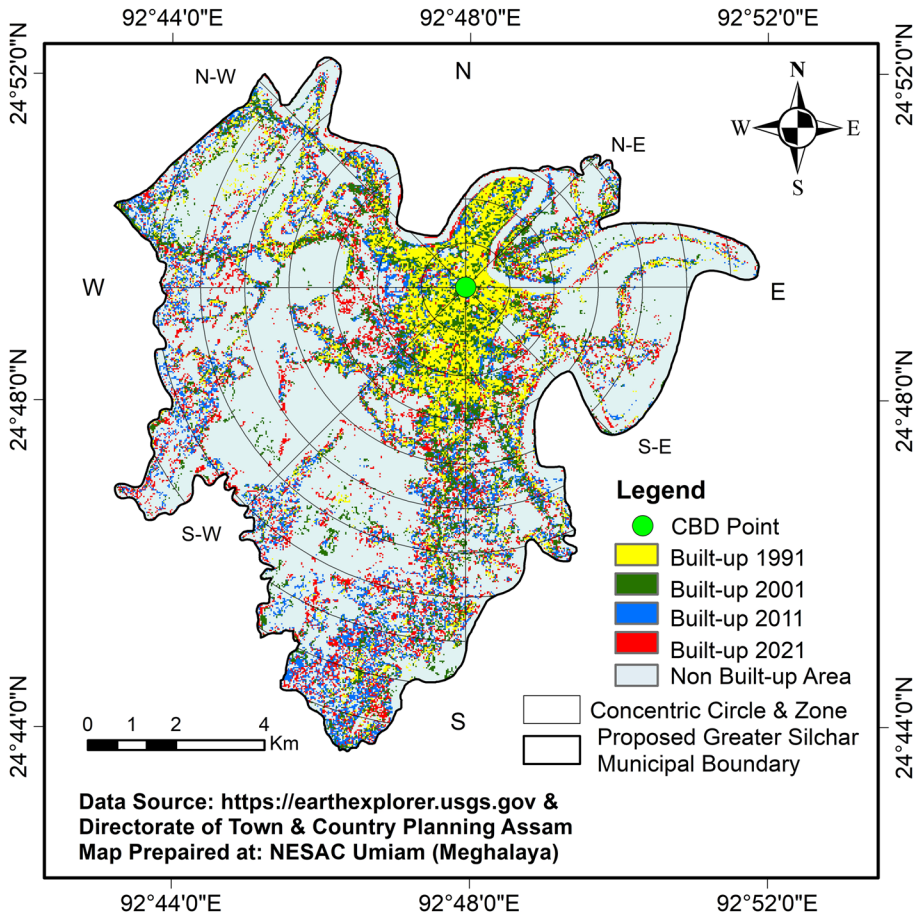
Fig. 10 Urban built-up growth of proposed GSC plan region from 1991 to 2021

with particular directions. Figure 13 exhibits the map of concentric circle-wise Shannon entropy values. The detailed descriptions of the gradient zone-wise total geographical land, urban built-up land, changes and the Shannon entropy values are attached in Appendix Table 3.

The maximum geographical land covered by zone V between the S-SW directions from CBD is nearly 3243.87 ha. Its built-up area has doubled in the last three decades as in 1991 built-up area recorded 266.58 ha, which rose to 824.31 ha in 2021. The trend shows the city's growth in this direction was increasing continuously. The major factor in attracting growth in this direction is almost plane surface, so the commercial and residential growth occurred on both sides of the highway, major roads and streets. The Silchar Medical College, numerous private hospitals, Polytechnic College, the National Institute of Technology (NIT Silchar) and other mixed built-up areas (commercial with residential) are present in this zone. The above facilities attract people for residential and commercial activities. The gradient zones (GZs) in the S-SW direction, GZs 26 to 32, have the area of the zone in increasing order, while the density of built-up settlements follows sprawling trends with increasing distance from the CBD. Here, the GZs 26, 27 and 28 were covered in 0 to 3 km

Table 1 Details of spatial direction-wise changes in built-up area and Shannon entropy from 1991 to 2021

Direction from CBD	Zone	Total area in ha	Built-up area in ha				Built-up area changes in ha				Shannon entropy values			
			1991	2001	2011	2021	1991–2001	2001–2011	2011–2021	1991–2021	1991	2001	2011	2021
N–NE	I	352.62	115.56	146.97	169.47	179.73	31.41	22.5	10.26	64.17	0.231	0.204	0.182	0.162
NE–E	II	927.45	69.66	102.78	119.7	142.2	33.12	16.92	22.5	72.54	0.182	0.177	0.159	0.154
E–SE	III	954.81	76.32	93.06	101.43	150.75	16.74	8.37	49.32	74.43	0.182	0.157	0.133	0.155
SE–S	IV	1141.56	140.85	218.88	276.3	341.82	78.03	57.42	65.52	200.97	0.313	0.252	0.313	0.311
S–SW	V	3243.87	266.58	460.26	682.47	824.31	193.68	222.21	141.84	557.73	0.562	0.646	0.705	0.693
SW–W	VI	2228.49	102.24	165.69	276.21	377.73	63.45	110.52	101.52	275.49	0.24	0.273	0.327	0.358
W–NW	VII	1950.39	176.4	259.11	315.72	389.34	82.71	56.61	73.62	212.94	0.397	0.389	0.362	0.361
NW–N	VIII	397.44	51.84	70.56	90.63	111.42	18.72	20.07	20.79	59.58	0.136	0.131	0.126	0.126
Grand Total		11,196.6	999.45	1517.31	2031.93	2517.3	517.86	514.62	485.37	1517.85	2.271	2.234	2.315	2.326

Table 2 Details of concentric circle-wise changes in a built-up area and Shannon entropy from 1991 to 2021

| Concentric circle	Total area in ha	Built-up area in ha				Built-up area changes in ha				Shannon entropy values			
		1991	2001	2011	2021	1991- 2001	2001- 2011	2011- 2021	1991–2021	1991	2001	2011	2021
1	313.47	170.19	185.67	208.44	226.62	15.48	22.77	18.18	56.43	0.393	0.303	0.264	0.237
2	884.34	281.70	358.56	404.37	462.24	76.86	45.81	57.87	180.54	0.563	0.422	0.436	0.412
3	1359.72	194.49	265.14	305.10	416.34	70.65	39.96	111.24	221.85	0.403	0.379	0.341	0.372
4	1625.76	105.30	170.28	217.26	303.84	64.98	46.98	86.58	198.54	0.259	0.274	0.265	0.291
5	1825.47	66.78	130.32	177.12	223.02	63.54	46.80	45.90	156.24	0.168	0.211	0.213	0.219
6	1746.45	63.18	127.44	164.25	224.10	64.26	36.81	59.85	160.92	0.166	0.206	0.199	0.215
7	1654.92	60.48	116.46	204.93	256.50	55.98	88.47	51.57	196.02	0.148	0.184	0.227	0.23
8	873.54	24.03	73.98	137.16	162.45	49.95	63.18	25.29	138.42	0.062	0.114	0.147	0.14
9	553.68	16.65	49.23	96.84	108.90	32.58	47.61	12.06	92.25	0.062	0.073	0.1	0.095
10	266.67	11.34	26.01	78.12	93.78	14.67	52.11	15.66	82.44	0.03	0.042	0.078	0.076
11	92.61	5.31	14.22	38.34	39.51	8.91	24.12	1.17	34.20	0.017	0.026	0.045	0.039
Grand Total	11,196.63	999.45	1517.31	2031.93	2517.30	517.86	514.62	485.37	1517.85	2.271	2.234	2.315	2.326
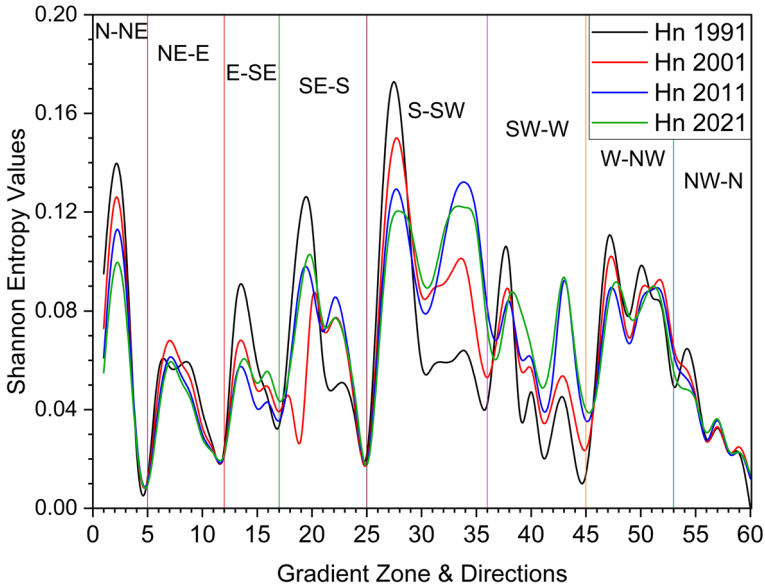
Fig. 11 Graphical representation of gradient zone-wise Shannon entropy values from 1991 to 2021

distance, indicating the entropy values were decreasing continuously, and the built-up area was following the infill growth trends. The GZs 29 to 31 have linear growth near the main roadside, while leapfrog growth was observed with increasing distance from the main road. The shape of the GZs 33 to 36 was in decreasing order, whereas the built-up growth and entropy values of these regions show a continuously increasing trend representing urban growth with a sprawl pattern. The NIT Silchar and Fakirtila market has come under the GZ 33 and been higher entropy, indicating the compactness of residential land, and leapfrog with infill developments follows. Some portion of the area in GZs 30 to 34 was nearly 4 to 5 m lower in altitude than the residential area, so during the monsoon, it gets submerged by water. That is why the built-up growth has not occurred in these low-lying areas.

Zone VI followed the same growth patterns in the W-SW direction, which covers 2228.49 ha of the total geographical area of the GSC. The 275.49 ha built-up infrastructure land growth has been observed in this region from 1991 to 2021. The entropy values of this zone were found to be 0.240, 0.273, 0.327 and 0.358 from 1991, 2001, 2011 and 2021, respectively. It represents the increasing trends in entropy values symbolizing urban sprawl. The GZs 37 and 38 are under 2 km distance and have followed infill type growth, while GZs 39 and 40, under 3 to 4 km distance from CBD, have linear growth near the major road and infill growth trends in the available open space within the residential area. GZs 41 and 42 have very few built-up areas, and most of the land is agricultural. The GZs 43 to 45 have some villages surrounded by agricultural land. The Shannon entropy values have continuously increased in GZs 38 to 45, indicating that their built-up area was increased from 1991 to 2021 but in an unorganized dispersed manner and nonlinear patterns.

Zone VII (W-NW) covers 1950.39 ha of the total geographical area. Here the observation found that the 212.94 ha of the built-up area has increased from 1991 to 2021, and the Shannon entropy has decreased with minor variation, indicating compact growth trends. In brief, the GZ 46 is within 1 km from CBD; most of the area here was covered
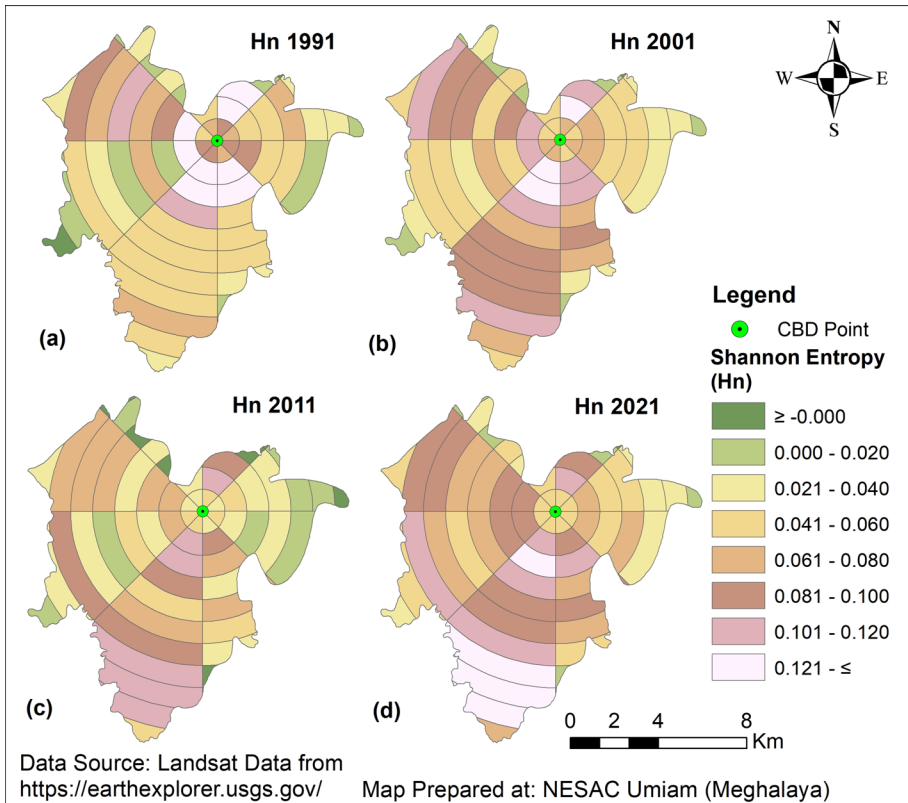
Fig. 12 Representation of changes in gradient zone-wise Shannon entropy values: **a** 1991, **b** 2001, **c** 2011 and **d** 2021

by cantonment, so no significant change has been recorded in the urban built-up class. The GZs 47 and 48, present 2 to 3 km from CBD, have observed the maximum built-up growth along the entire area in this direction. The Silchar railway station is located in the GZ 47, so the mixed built-up land, commercial and residential area, has grown continuously following the infill growth trend. GZ 48 is primarily residential, with a small portion of land covered by commercial, industrial and warehouses, which has been growing since 2001, while the Shannon entropy values have been observed at a minimum in 2011. The mixed growth pattern types have been followed across all GZs in this direction.

The S-SE direction has zone IV and covers a 1141.56 ha area of about 200.97 ha of built-up land expanded from 1991 to 2021. The Shannon entropy value was the minimum in 2001, while the remaining period shows slight variation. The GZs 18, 19 and 20 in under 3 km distance from the CBD, where most of the land shows the compact and infill growth trends followed by the commercial, mixed built-up areas and residential areas. The GZ 21 has a sprawl trend with linear growth near the highway. In GZs 22 to 25, an uneven built-up growth pattern was followed by leapfrog and scattered growth trends.

Zone III (E-SE) covers a total area of around 954.81 ha, and approximately 74.43 ha of the built-up area increased from 1991 to 2021. The Shannon entropy values were 0.182, 0.157, 0.133 and 0.154 during 1991 to 2021. The GZ 13 nearest to the CBD was
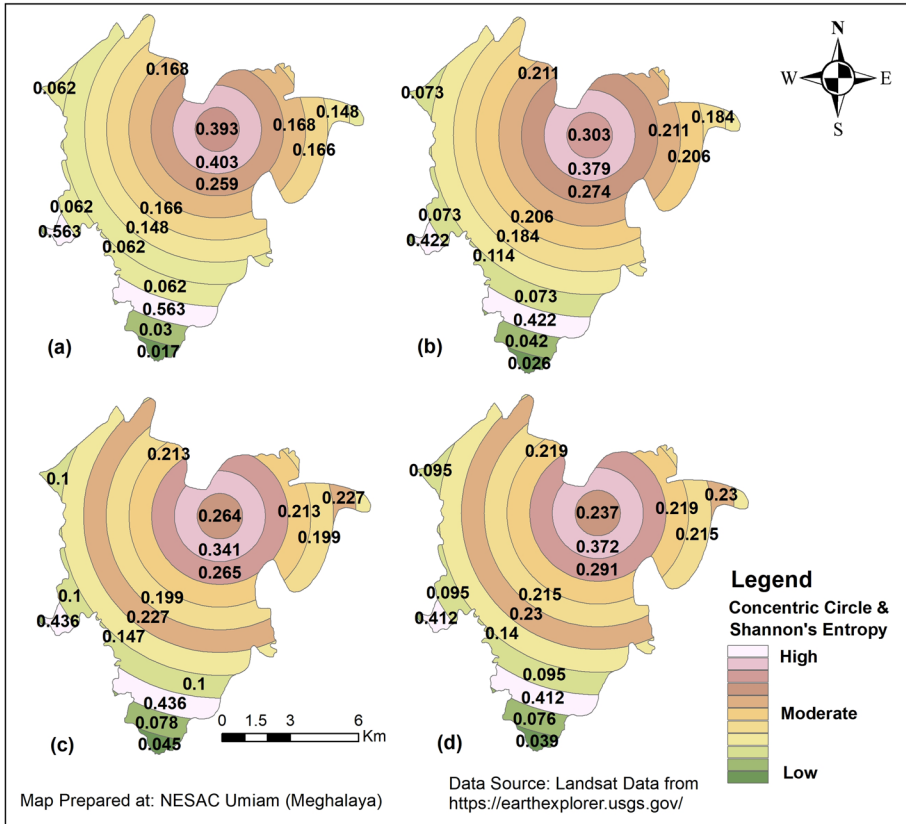
Fig. 13 Representation of changes in concentric circle-wise Shannon entropy values from 1991 to 2021

densely populated and had a compact built-up landscape. The commercial activities are found in practice across the major roads and inner area of this zone and the residential land. The infill and organized urban growth pattern was noticed here. The GZs 14 and 15 are 2–3 km from the CBD and have been built-up growth continuously, but the rate was lower than GZ 13. The Shannon entropy values decrease continuously, and mostly leapfrog growth has been found in all GZ in this zone. Only the GZ 17 covers by agricultural land with the river in the east direction.

The E-NE direction has zone II with a 927.45 ha total area and 142.2 ha of total built-up land in 2021, which was 69.66 ha in 1991. The entropy values observed 0.182, 0.177, 0.159 and 0.154 in 1991, 2001, 2011 and 2021, respectively. It is an indication that the built-up area has grown continuously. The GZ 6 is under 1 km from CBD and has dense built-up, including commercial, residential and official areas with some portion of the Barak River. The GZs 7 and 8 from 2 to 3 km from CBD have a high built-up growth rate, and the entropy values also increased continuously. The growth pattern in this area is linear near the roadsides, but far from the major roads; it has an unorganized, scattered and leapfrog urban growth type. The GZs 9 to 12 have rural areas and a slower rate of built-up growth with scattered trends.

The N-NW direction under zone VIII covered 397.44 ha of the total area, while the built-up land was 111.42 ha in 2021. The maximum area of this zone is covered by the Barak River, which creates the outer boundary of this zone. The built-up growth in this region has around 59.58 ha from 2001 to 2021, which was a comparatively slower rate of urban growth. The entropy values found in decreasing trends may indicate sprawled and scattered growth. The GZ 54 is near the city centre, having most of the area covered by official and recreational areas, and the built-up growth was much slower due to the lack of available open space and vacant land. The GZ 55 covers a tiny portion of the river and residential area, rising to compactness with the growth of most of the infill types. The GZs 56 and 57 have observed linear growth on both sides of the major road and infill growth with low built-up density. The river has covered the maximum land of the GZs 58 and 60 with small patches of built-up land. At the same time, the GZ 59 has a meandering river, and the built-up area follows the river pattern through infill growth with minor variations in entropy values.

Zone I (N-NE) covers the minimum portion of the total geographical land of only 352.62 ha. The built-up land in 1991, 2001, 2011 and 2021 was approximately 115.56 ha, 146.97 ha, 169.47 ha and 179.73 ha, while the Shannon entropy values were 0.231, 0.203, 0.182 and 0.162, respectively. The GZs 1, 2 and 3 are covered under the old city area, and the entropy values show decreasing trends, representing the built-up area grown to compact with the infill growth type. The GZ 4 has a minor built-up area, while no built-up patches were found in GZ 5.

The detailed statistics of concentric circle-wise changes in a built-up area and Shannon entropy from 1991 to 2021 are given in Table 2 and Fig. 13. The concentric circle (CC) 1 covers a 313.47 ha area, while the built-up growth from 1991 to 2021 is 170.19 ha to 226.62 ha and entropy values were 0.393 to 0.237. The CC 1 is dense and compact from the N to W clockwise directions means the urban growth occurs continuously here within following maximum infill growth trends. At the same time, most of the portion of the W–N direction has been utilized for cantonment and recreational activities, so there are fewer built-up area increments in this direction. Ring 2 covers an 884.34 ha area, and built-up land growth occurred in all directions. The entropy values decreased continuously from 0.562 to 0.411, indicating the area was moving to compactness. Ring 3 observed the built-up patches almost in all directions, while N-NE and SE-SW are more compact than in the other directions. Rings 4, 5 and 8 observed the maximum built-up growth towards the SE to SW directions, while rings 6, 7, 9, 10 and 11 follow the sprawled and dispersed built-up growth patterns in all directions.

5 Conclusion

The present research study is focused on the urban built-up area growth dynamics from 1991 to 2021 using land use data of the Greater Silchar City (GSC) plan region. It demonstrates that integrated GIS techniques such as spatial directions, concentric circles and gradient zonal approaches with landscape metrics and Shannon entropy models are powerful tools. They are suitable for analysing and monitoring urban growth patterns in every nook and corner of the city limits. Shannon entropy variables have been employed to measure the extent of urban growth and the fractal value to understand the dynamics of change in the fractal aspect of sprawl.

- Except for the core area, the built-up area was scattered randomly and rises with increasing distance from the city's centre. Most of the unoccupied lands are being converted into residential, commercial, mixed built-up areas on day by day. The urban

growth and sprawl process are ongoing in all directions of the GSC region. Most of the rapid built-up growth has happened in areas between 8 and 11 km distance from CBD and under the S-SW directions.

- Maximum infill growth trends have been observed under a 2 km distance from the central business district (CBD). The linear built-up growth pattern has followed most of the highways and major roads. But mixed growth patterns of linear, scattered, infill and leapfrog have been found in the areas with a distance of over 3 km. The built-up growth varies with various conditions such as direction, available space, road network and geomorphological conditions.

- Integrating the GIS technique with built-up land use data and the spatial direction approach applied to FRAGSTATS v4.2 software has provided precise results for urban landscape patterns. The landscape metrics deal with edge, patch, shape and aggregation metrics, which helps to understand the growth pattern of built-up land. The core area, total edge, number of patches, LSI and Shannon entropy had maximum values in the S-SW direction representing the maximum built-up growth, whereas in the case of the radial distance from CBD, ring 3 has the highest built-up growth. Patch densities were higher in N-NE, S-SE and N-NW directions, indicating a higher and more compact built-up growth rate.

- The minimum built-up growth of 56.43 ha has been found under 1 km from CBD, with entropy changing from 0.393 to 0.237, whereas in the N-NE direction, built-up growth is 64.17 ha, with entropy changing from 0.2314 to 0.1624 within the years 1991 to 2021. The reason is that both regions were under the older township, which is already densely populated and has minimal availability of vacant lands.

- Shannon entropy results show that the city has compacted near the centre while the dispersion rate of built-up areas has been rising, ultimately demonstrating that the process of urban expansion has been happening continuously. In the study area, the built-up patterns follow an unsystematic and imbalanced growth over different periods and directions.

- The present study recommends the policymaker of Greater Silchar City to improve the road network and facilities of public transportation, which will help in reducing the problem of traffic congestion. New built-up (residential, colonies, commercial, official, institutional, medical, etc.) projects should be set up on the outskirts of the city. This can help maintain the goals of sustainable development and reduce the pressure of overcrowding in the city's core area. This research can help to find out the available vacant landscapes and periodic built-up growth trends in particular directions and distances from CBD.

In general, utilizing spatial–temporal data and quantitative methods within the framework of remote sensing (RS) and geographical information systems (GIS) proves to be an effective strategy for analysing urban growth trends. These modelling approaches can be employed to delineate growth patterns for any city. The methods proposed in this research hold significant benefits for researchers, municipal bodies and decision-makers involved in the development of sustainable urban planning strategies. Ultimately, this study recommends the integration of RS spatial–temporal data, GIS tools and quantitative approaches, such as the Shannon entropy model and landscape metrics, to encourage a more comprehensive understanding of the urban environment.

Appendix

See Table 3.

Table 3 Details of gradient zone-wise changes in built-up area and Shannon entropy from 1991 to 2021

Gradient zone	Total area in ha	Built-up area in ha				Built-up area changes in ha				Shannon entropy values			
		1991	2001	2011	2021	1991–2001	2001–2011	2011–2021	1991–2021	1991	2001	2011	2021
1	40.14	25.92	27.63	28.8	31.32	1.71	1.17	2.52	5.4	0.095	0.073	0.061	0.055
2	119.07	51.39	69.75	77.22	80.37	18.36	7.47	3.15	28.98	0.153	0.142	0.125	0.11
3	152.82	37.71	46.17	57.78	60.39	8.46	11.61	2.61	22.68	0.124	0.107	0.102	0.09
4	38.61	0.36	3.06	5.13	6.75	2.7	2.07	1.62	6.39	0.003	0.013	0.016	0.016
5	1.98	0.18	0.36	0.54	0.9	0.18	0.18	0.36	0.72	0.002	0.002	0.003	0.003
6	38.25	16.92	18.99	19.8	21.6	2.07	0.81	1.8	4.68	0.07	0.055	0.046	0.041
7	116.91	12.15	27.9	32.49	40.14	15.75	4.59	7.65	27.99	0.054	0.074	0.067	0.066
8	195.3	13.23	19.71	23.94	27.81	6.48	4.23	3.87	14.58	0.058	0.057	0.053	0.05
9	254.34	14.49	18.9	21.33	24.75	4.41	2.43	3.42	10.26	0.062	0.055	0.048	0.046
10	171.09	7.38	8.37	10.08	11.7	0.99	1.71	1.62	4.32	0.037	0.029	0.027	0.025
11	103.86	4.68	7.2	8.73	11.07	2.52	1.53	2.34	6.39	0.026	0.026	0.024	0.024
12	47.7	0.81	1.71	3.33	5.13	0.9	1.62	1.8	4.32	0.006	0.008	0.011	0.013
13	40.5	26.73	27.63	28.98	32.31	0.9	1.35	3.33	5.58	0.097	0.073	0.061	0.056
14	119.25	23.94	24.66	26.64	38.88	0.72	1.98	12.24	14.94	0.09	0.067	0.057	0.065
15	195.21	11.97	13.05	13.77	23.58	1.08	0.72	9.81	11.61	0.053	0.041	0.034	0.044
16	257.58	10.44	19.17	21.78	37.62	8.73	2.61	15.84	27.18	0.048	0.056	0.049	0.063
17	342.27	3.24	8.55	10.26	18.36	5.31	1.71	8.1	15.12	0.019	0.03	0.027	0.036
18	38.43	19.35	20.88	25.83	30.6	1.53	4.95	4.77	11.25	0.077	0.059	0.056	0.054
19	117.09	39.33	54.36	58.5	62.64	15.03	4.14	4.14	23.31	0.128	0.12	0.103	0.092
20	191.34	40.41	48.96	53.01	83.34	8.55	4.05	30.33	42.93	0.13	0.111	0.096	0.113
21	164.16	9.63	21.51	28.08	38.43	11.88	6.57	10.35	28.8	0.045	0.061	0.06	0.064
22	205.74	10.44	32.13	52.02	53.1	21.69	19.89	1.08	42.66	0.048	0.082	0.094	0.082
23	237.96	12.24	26.91	37.53	42.84	14.67	10.62	5.31	30.6	0.054	0.072	0.074	0.07
24	158.04	7.83	11.88	18.27	25.47	4.05	6.39	7.2	17.64	0.038	0.038	0.043	0.047
25	28.8	1.62	2.25	3.06	5.4	0.63	0.81	2.34	3.78	0.011	0.01	0.01	0.014

Table 3 (continued)

Gradient zone	Total area in ha	Built-up area in ha				Built-up area changes in ha				Shannon entropy values			
		1991	2001	2011	2021	1991–2001	2001–2011	2011–2021	1991–2021	1991	2001	2011	2021
26	38.16	24.75	27.27	32.22	33.66	2.52	4.95	1.44	8.91	0.092	0.073	0.066	0.058
27	116.91	65.61	71.91	79.74	90.72	6.3	7.83	10.98	25.11	0.179	0.145	0.128	0.12
28	195.12	62.19	80.73	84.33	91.8	18.54	3.6	7.47	29.61	0.173	0.157	0.133	0.121
29	273.87	30.15	50.58	59.67	88.02	20.43	9.09	28.35	57.87	0.106	0.114	0.104	0.118
30	352.35	9.81	29.97	38.16	58.59	20.16	8.19	20.43	48.78	0.046	0.078	0.075	0.088
31	430.56	13.86	36.9	42.12	58.23	23.04	5.22	16.11	44.37	0.06	0.091	0.081	0.088
32	508.95	13.5	36.09	61.83	83.88	22.59	25.74	22.05	70.38	0.059	0.089	0.107	0.114
33	515.07	13.59	41.04	81.81	94.95	27.45	40.77	13.14	81.36	0.059	0.098	0.13	0.124
34	453.6	16.47	45.54	86.13	91.17	29.07	40.59	5.04	74.7	0.068	0.106	0.134	0.121
35	266.67	11.34	26.01	78.12	93.78	14.67	52.11	15.66	82.44	0.051	0.07	0.126	0.123
36	92.61	5.31	14.22	38.34	39.51	8.91	24.12	1.17	34.2	0.028	0.044	0.075	0.066
37	40.14	24.48	26.82	28.62	29.52	2.34	1.8	0.9	5.04	0.091	0.072	0.061	0.053
38	118.71	37.89	43.83	54.72	65.16	5.94	10.89	10.44	27.27	0.125	0.103	0.098	0.095
39	197.19	1.17	13.5	22.23	52.74	12.33	8.73	30.51	51.57	0.008	0.043	0.05	0.081
40	275.67	16.11	24.75	35.37	40.59	8.64	10.62	5.22	24.48	0.067	0.068	0.071	0.067
41	353.88	0.9	6.84	12.6	21.42	5.94	5.76	8.82	20.52	0.007	0.025	0.032	0.041
42	432.9	6.93	14.58	19.44	36.36	7.65	4.86	16.92	29.43	0.035	0.045	0.045	0.062
43	498.69	12.24	21.15	66.78	79.92	8.91	45.63	13.14	67.68	0.054	0.06	0.113	0.11
44	211.23	2.34	10.53	25.74	34.29	8.19	15.21	8.55	31.95	0.015	0.035	0.056	0.059
45	100.08	0.18	3.69	10.71	17.73	3.51	7.02	7.02	17.55	0.002	0.015	0.028	0.035
46	37.89	14.04	15.66	19.44	21.15	1.62	3.78	1.71	7.11	0.06	0.048	0.045	0.041
47	115.65	38.61	49.95	53.82	58.23	11.34	3.87	4.41	19.62	0.126	0.113	0.097	0.088
48	193.95	24.75	38.34	44.1	66.42	13.59	5.76	22.32	41.67	0.092	0.093	0.084	0.096
49	273.42	16.02	19.26	26.28	44.55	3.24	7.02	18.27	28.53	0.067	0.056	0.057	0.072

Table 3 (continued)

Gradient zone	Total area in ha	Built-up area in ha				Built-up area changes in ha				Shannon entropy values			
		1991	2001	2011	2021	1991–2001	2001–2011	2011–2021	1991–2021	1991	2001	2011	2021
50	351.54	31.95	40.14	48.15	51.39	8.19	8.01	3.24	19.44	0.111	0.097	0.089	0.08
51	430.92	19.89	33.12	46.44	63.36	13.23	13.32	16.92	43.47	0.078	0.084	0.087	0.093
52	428.58	24.66	42.48	50.94	56.43	17.82	8.46	5.49	31.77	0.092	0.101	0.093	0.086
53	118.44	6.48	20.16	26.55	27.81	13.68	6.39	1.26	21.33	0.033	0.058	0.057	0.05
54	39.96	18	20.79	24.75	26.46	2.79	3.96	1.71	8.46	0.073	0.059	0.054	0.048
55	60.75	12.78	16.2	21.24	26.1	3.42	5.04	4.86	13.32	0.056	0.049	0.048	0.048
56	38.79	3.06	4.68	5.94	10.26	1.62	1.26	4.32	7.2	0.018	0.018	0.018	0.023
57	88.11	8.1	13.05	19.62	23.13	4.95	6.57	3.51	15.03	0.04	0.041	0.045	0.044
58	46.62	2.88	3.96	5.31	7.56	1.08	1.35	2.25	4.68	0.017	0.016	0.016	0.018
59	110.25	5.58	8.73	9.99	12.24	3.15	1.26	2.25	6.66	0.029	0.03	0.027	0.026
60	12.96	1.44	3.15	3.78	5.67	1.71	0.63	1.89	4.23	0.01	0.013	0.012	0.014
Total	11,197	999.45	1517.31	2031.9	2517.3	517.9	514.6	485.37	1517.9	3.755	3.868	3.889	3.91

Declarations

References

Akhter, S. T., & Noon, M. H. (2016). Modeling spillover effects of leapfrog development and urban sprawl upon institutional delinquencies: A case for Pakistan. *Procedia - Social and Behavioral Sciences, 216*, 279–294. https://doi.org/10.1016/j.sbspro.2015.12.039

Altieri, L., Cocchi, D., & Roli, G. (2019). Advances in spatial entropy measures. *Stochastic Environmental Research and Risk Assessment, 33*(4–6), 1223–1240. https://doi.org/10.1007/s00477-019-01686-y

Anees, M. M., Sajjad, S., & Joshi, P. K. (2019). Characterizing urban area dynamics in historic city of Kurukshetra, India, using remote sensing and spatial metric tools. *Geocarto International, 34*(14), 1584–1607. https://doi.org/10.1080/10106049.2018.1499819

Ashwini, K., & Sil, B. S. (2019). Analysis and estimation of the rainfall trend in the North-East India. *Journal of Energy Research and Environmental Technology (JERET), 6*, 96–100.

Azhdari, A., Taghvaee, A. A., & Kheyroddin, R. (2018). Spatiotemporal analysis of Shiraz metropolitan area expansion during 1986–2014: Using remote sensing imagery and landscape metrics. *TT Iust, 28*(2), 163–173. https://doi.org/10.22068/ijaup.28.2.163

Bhat, P. A., Shafiq, M., Mir, A. A., & Ahmed, P. (2017). Urban sprawl and its impact on landuse/land cover dynamics of Dehradun City, India. *International Journal of Sustainable Built Environment, 6*(2), 513–521. https://doi.org/10.1016/j.ijsbe.2017.10.003

Burgess, E. W. (2015). The growth of the city: an introduction to a research project. In *The city reader* (pp. 212–220). Routledge. https://doi.org/10.1007/978-0-387-73412-5_5

Cegielska, K., Kukulska-Kozieł, A., Salata, T., Piotrowski, P., & Szylar, M. (2018). Shannon entropy as a peri-urban landscape metric: Concentration of anthropogenic land cover element. *Journal of Spatial Science, 64*(3), 469–489. https://doi.org/10.1080/14498596.2018.1482803

Chatterjee, N. D., Chatterjee, S., & Khan, A. (2016). Spatial modeling of urban sprawl around Greater Bhubaneswar city, India. *Modeling Earth Systems and Environment, 2*, 1–21. https://doi.org/10.1007/s40808-015-0065-7

Chettry, V., & Surawar, M. (2020). Urban sprawl assessment in Raipur and Bhubaneswar urban agglomerations from 1991 to 2018 using geoinformatics. *Arabian Journal of Geosciences, 13*(667), 1–17. https://doi.org/10.1007/s12517-020-05693-0

Chettry, V., & Surawar, M. (2021). Urban sprawl assessment in eight mid-sized Indian Cities using RS and GIS. *Journal of the Indian Society of Remote Sensing, 49*(11), 2721–2740. https://doi.org/10.1007/s12524-021-01420-8

Das, S., Adhikary, P. P., Shit, P. K., & Bera, B. (2021). Urban wetland fragmentation and ecosystem service assessment using integrated machine learning algorithm and spatial landscape analysis. *Geocarto International, 37*(25), 7800–7818. https://doi.org/10.1080/10106049.2021.1985174

Das, S., & Angadi, D. P. (2021). Assessment of urban sprawl using landscape metrics and Shannon's entropy model approach in town level of Barrackpore sub-divisional region, India. *Modeling Earth Systems and Environment, 7*, 1071–1095. https://doi.org/10.1007/s40808-020-00990-9

Deribew, K. T. (2020). Spatiotemporal analysis of urban growth on forest and agricultural land using geospatial techniques and Shannon entropy method in the satellite town of Ethiopia, the western fringe of Addis Ababa city. *Ecological Processes*. https://doi.org/10.1186/s13717-020-00248-3

Dhali, M. K., Chakraborty, M., & Sahana, M. (2019). Assessing spatio-temporal growth of urban sub-centre using Shannon's entropy model and principle component analysis: A case from North 24 Parganas, lower Ganga River Basin, India. *Egyptian Journal of Remote Sensing and Space Science, 22*(1), 25–35. https://doi.org/10.1016/j.ejrs.2018.02.002

Dhanaraj, K., & Angadi, D. P. (2020). Land use land cover mapping and monitoring urban growth using remote sensing and GIS techniques in Mangaluru, India. *GeoJournal, 4*, 1–27. https://doi.org/10.1007/s10708-020-10302-4

Dhanaraj, K., & Angadi, D. P. (2021). Urban expansion quantification from remote sensing data for sustainable land-use planning in Mangaluru, India. *Remote Sensing Applications: Society and Environment, 23*, 100602. https://doi.org/10.1016/j.rsase.2021.100602

Dhanaraj, K., & Angadi, D. P. (2022). Analysis of urban expansion patterns through landscape metrics in an emerging metropolis of Mangaluru community development block, India, during 1972–2018. *Journal of the Indian Society of Remote Sensing, 50*, 1855–1870. https://doi.org/10.1007/s12524-022-01567-y

Du, L., Li, X., Yang, M., Sivakumar, B., Zhu, Y., Pan, X., Li, Z., & Sang, Y. F. (2022). Assessment of spatiotemporal variability of precipitation using entropy indexes: A case study of Beijing, China. *Stochastic Environmental Research and Risk Assessment, 36*(4), 939–953. https://doi.org/10.1007/s00477-021-02116-8

Farooq, M., & Muslim, M. (2014). Dynamics and forecasting of population growth and urban expansion in Srinagar city: A geospatial approach. *International Archives of the Photogrammetry, Remote Sensing and Spatial Information Sciences, ISPRS Technical Commission VIII Symposium, 09 – 12 December 2014, XL–8*, 709–716. https://doi.org/10.5194/isprsarchives-XL-8-709-2014

Feng, L., & Li, H. (2012). Analysis of urban sprawl: Case study of Jiangning, Nanjing, China. *Journal of Urban Planning and Development, 138*(3), 263–269. https://doi.org/10.1061/(asce)up.1943-5444.0000119

Frazier, A. E., & Kedron, P. (2017). Landscape metrics: Past progress and future directions, current landscape ecology reports. *Current Landscape Ecology Reports, 2*(3), 63–72. https://doi.org/10.1007/s40823-017-0026-0

Harig, O., Hecht, R., Burghardt, D., & Meinel, G. (2021). Automatic delineation of urban growth boundaries based on topographic data using germany as a case study. *ISPRS International Journal of Geo-Information, 10*(5), 353–384. https://doi.org/10.3390/ijgi10050353

Horo, J. P., & Punia, M. (2019). Urban dynamics assessment of Ghaziabad as a suburb of National Capital Region, India. *GeoJournal, 84*, 623–639. https://doi.org/10.1007/s10708-018-9877-0

Ilyassova, A., Kantakumar, L. N., & Boyd, D. (2021). Urban growth analysis and simulations using cellular automata and geo-informatics: Comparison between Almaty and Astana in Kazakhstan. *Geocarto International, 36*(5), 520–539. https://doi.org/10.1080/10106049.2019.1618923

Jaafari, S., Sakieh, Y., Shabani, A. A., Danehkar, A., & Nazarisamani, A. A. (2016). Landscape change assessment of reservation areas using remote sensing and landscape metrics (case study: Jajroud reservation, Iran). *Environment, Development and Sustainability, 18*(6), 1701–1717. https://doi.org/10.1007/s10668-015-9712-4

Jahani, N., & Barghjelveh, S. (2021). Urban landscape services planning in an urban river-valley corridor system case study: Tehran's Farahzad River-valley landscape system. *Environment, Development and Sustainability, 24*, 867–887. https://doi.org/10.1007/s10668-021-01474-1

Jain, S., Kohli, D., Rao, R. M., & Bijker, W. (2011). Spatial metrics to analyse the impact of regional factors on pattern of urbanisation in Gurgaon, India. *Journal of the Indian Society of Remote Sensing, 39*, 203–212. https://doi.org/10.1007/s12524-011-0088-0

Jat, M. K., Garg, P. K., & Khare, D. (2008). Modelling of urban growth using spatial analysis techniques: A case study of Ajmer city (India). *International Journal of Remote Sensing, 29*(2), 543–567. https://doi.org/10.1080/01431160701280983

Kowe, P., Pedzisai, E., Gumindoga, W., & Rwasoka, D. T. (2015). An analysis of changes in the urban landscape composition and configuration in the Sancaktepe District of Istanbul Metropolitan City, Turkey using landscape metrics and satellite data. *Geocarto International, 30*(5), 506–519. https://doi.org/10.1080/10106049.2014.905638

Kumar, S., Shwetank, N., & Jain, K. (2020). A multi-temporal landsat data analysis for land-use/land-cover change in Haridwar region using remote sensing techniques. *Procedia Computer Science, 171*, 1184–1193. https://doi.org/10.1016/j.procs.2020.04.127

Liu, P., Jia, S., Han, R., Liu, Y., Lu, X., & Zhang, H. (2020). RS and GIS supported urban LULC and UHI change simulation and assessment. *Journal of Sensors, 2020*, 1–17. https://doi.org/10.1155/2020/5863164

Malarvizhi, K., Kumar, S. V., & Porchelvan, P. (2022). Urban sprawl modelling and prediction using regression and Seasonal ARIMA: A case study for Vellore, India. *Modeling Earth Systems and Environment, 8*, 1597–1615. https://doi.org/10.1007/s40808-021-01170-z

Mandal, S., Kundu, S., Haldar, S., Bhattacharya, S., & Paul, S. (2020). Monitoring and measuring the urban forms using spatial metrics of Howrah City India. *Remote Sensing of Land, 4*(1–2), 19–39. https://doi.org/10.21523/gcj1.20040103

Mandal, V. P., Shutrana, S., Pandey, P. C., Patairiya, S., Shamim, M., Sharma, S., & Tomar, V. (2014). Appraisal of suitability for urban planning and expansion analysis using quick bird satellite data. *ARPN Journal of Engineering and Applied Sciences, 9*(12), 2716–2722.

McGarigal, K., & Marks, B. J. (1995). FRAGSTATS: Spatial pattern analysis program for quantifying landscape structure. In *General Technical Report (GTR)*. U.S. Department of Agriculture, Forest Service, Pacific Northwest Research Station. https://doi.org/10.2737/PNW-GTR-351

Mishra, M., Mishra, K., Subudhi, A., & Phil, M. (2011). Urban Sprawl mapping and land use change analysis using remote sensing and GIS (Case Study of Bhubaneswar City, Orissa). *Proceedings of the Geo-Spatial World Forum ….*

Mithun, S., Sahana, M., Chattopadhyay, S., Johnson, B. A., Khedher, K. M., & Avtar, R. (2021). Monitoring metropolitan growth dynamics for achieving sustainable urbanization (SDG 11.3) in Kolkata Metropolitan Area India. *Remote Sensing, 13*(21), 4423. https://doi.org/10.3390/rs13214423

Mohabey, D. P., & Kumar, A. (2015). Land use land cover exploration and change revealing in devghar district part of Jharkhand using multi-temporal satellite data. *Journal of Remote Sensing & GIS, 6*(2), 1–12.

Mohabey, D. P., Lamay, B. J., Nishi, J. K., Sharma, N. K., & Kumar, A. (2015). Land use land cover analysis of Santhal Pargana using remote sensing. *Journal of Remote Sensing & Earth Science, 1*(1), 1–14.

Mohabey, D. P., Nongkynrih, J. M., & Kumar, U. (2023). Spatio-temporal analysis of land use/land cover change and urban growth dynamics of Silchar City, India using very high-resolution satellite data and the Shannon entropy model. *Land Degradation & Development*. https://doi.org/10.1002/ldr.4608

Mohamed, M. A. (2017). Monitoring of temporal and spatial changes of land use and land cover in metropolitan regions through remote sensing and GIS. *Natural Resources, 8*, 353–369. https://doi.org/10.4236/nr.2017.85022

Mohammady, S., & Delavar, M. R. (2016). Urban sprawl assessment and modeling using landsat images and GIS. *Modeling Earth Systems and Environment, 2*, 1–14. https://doi.org/10.1007/s40808-016-0209-4

Nagendra, H., Munroe, D. K., & Southworth, J. (2004). From pattern to process: Landscape fragmentation and the analysis of land use/land cover change. *Agriculture, Ecosystems and Environment, 101*, 111–115. https://doi.org/10.1016/j.agee.2003.09.003

Narmada, K., Gogoi, D., & Dhanusree, G. B. (2021). Landscape metrics to analyze the forest fragmentation of Chitteri Hills in Eastern Ghats, Tamil Nadu. *Journal of Civil Engineering and Environmental Science*. https://doi.org/10.17352/2455-488x.000038

Nath, A., & Ghosh, S. (2022). Meandering rivers' morphological changes analysis and prediction—A case study of Barak river Assam. *H2Open Journal, 5*(2), 289–306. https://doi.org/10.2166/h2oj.2022.003

Noor, N. M., Asmawi, M. Z., & Rusni, N. A. (2014). Measuring urban sprawl on geospatial indices characterized by leap frog development using remote sensing and GIS techniques. *IOP Conference Series Earth and Environmental Science, 18*, 012174. https://doi.org/10.1088/1755-1315/18/1/012174

Patra, P. K., Behera, D., & Goswami, S. (2022). Relative Shannon's Entropy approach for quantifying urban growth using Remote Sensing and GIS: A case study of Cuttack City, Odisha, India. *Journal of the Indian Society of Remote Sensing, 50*(4), 747–762. https://doi.org/10.1007/s12524-022-01493-z

Pawe, C. K., & Saikia, A. (2020). Decumbent development : Urban sprawl in the Guwahati Metropolitan Area, India. *Singapore Journal of Tropical Geography, 41*, 226–247. https://doi.org/10.1111/sjtg.12317

Pourghasemi, H. R., Pradhan, B., & Gokceoglu, C. (2012). Remote sensing data derived parameters and its use in landslide susceptibility assessment using shannon's entropy and GIS. *Applied Mechanics and Materials, 225*, 486–491. https://doi.org/10.4028/www.scientific.net/AMM.225.486

Punia, M., & Singh, L. (2012). Entropy approach for assessment of urban growth: A case study of Jaipur, India. *Journal of the Indian Society of Remote Sensing, 40*(2), 231–244. https://doi.org/10.1007/s12524-011-0141-z

Rastogi, K., & Jain, G. V. (2018). Urban sprawl analysis using Shannon's entropy and fractal analysis: A case study on Tiruchirappalli City, India. *The International Archives of the Photogrammetry, Remote Sensing and Spatial Information Sciences, 42*(5), 761–766. https://doi.org/10.5194/isprs-archives-xlii-5-761-2018

Rath, S. S., Mohanty, S., & Panda, J. (2022). Analyzing the fragmentation of urban footprints in eastern and southern Indian Cities and driving factors. *Journal of the Indian Society of Remote Sensing, 50*(8), 1499–1517. https://doi.org/10.1007/s12524-022-01546-3

Reddy, A. (2017). Land use land cover change detection on Kanchinegalur sub watershed using GIS and Remote Sensing technique. *International Journal for Research in Applied Science and Engineering Technology, 5*(11), 2128–2136. https://doi.org/10.22214/ijraset.2017.11306

Saha, A., Nath, A., & Dey, A. K. (2022). Multivariate geophysical index-based prediction of the compression index of fine-grained soil through nonlinear regression. *Journal of Applied Geophysics, 204*, 104706. https://doi.org/10.1016/J.JAPPGEO.2022.104706

Saini, R., Aswal, P., Tanzeem, M., & Sanyam, S. S. (2019). Land use land cover change detection using remote sensing and GIS in Srinagar, India. *International Journal of Computer Applications, 178*(46), 42–50.

Sharma, N., Kullu, N. J., & Anshula, K. (2020). Spatiotemporal analysis of wetlands in Ranchi urban area, Jharkhand: Proposed national level urban wetland census. *Journal of Water Resource Engineering and Management, 7*(3), 16–22.

Shifaw, E., Sha, J., & Li, X. (2020). Detection of spatiotemporal dynamics of land cover and its drivers using remote sensing and landscape metrics (Pingtan Island, China). *Environment, Development and Sustainability, 22*, 1269–1298. https://doi.org/10.1007/s10668-018-0248-2

Shikary, C., & Rudra, S. (2021). Measuring urban land use change and sprawl using geospatial techniques: A study on Purulia Municipality, West Bengal, India. *Journal of the Indian Society of Remote Sensing, 49*(2), 433–448. https://doi.org/10.1007/s12524-020-01212-6

Shukla, A., & Jain, K. (2019). Critical analysis of spatial-temporal morphological characteristic of urban landscape. *Arabian Journal of Geosciences*. https://doi.org/10.1007/s12517-019-4270-y

Singh, B., & Sarkar, C. (2020). Monitoring urban growth and detection of land use/ land cover change in Silchar city, Assam and Balurghat city, West Bengal. *International Journal of Innovative Technology and Exploring Engineering, 9*(8), 796–803. https://doi.org/10.35940/ijitee.h6656.069820

Thakur, P. K., Kumar, M., & Gosavi, V. E. (2020). Monitoring and modelling of urban sprawl using geospatial techniques—A case study of Shimla City, India. In S. Sahdev, R. B. Singh, & M. Kumar (Eds.), *Geoecology of landscape dynamics. Advances in geographical and environmental sciences* (pp. 263–294). Singapore: Springer. https://doi.org/10.1007/978-981-15-2097-6_17

Tian, Y., & Chen, J. (2021). Suburban sprawl measurement and landscape analysis of cropland and ecological land: A case study of Jiangsu Province, China. *Growth and Change, 53*(3), 1282–1305. https://doi.org/10.1111/grow.12608

Toosi, N. B., Soffianian, A. R., Fakheran, S., & Waser, L. T. (2022). Mapping disturbance in mangrove ecosystems: Incorporating landscape metrics and PCA-based spatial analysis. *Ecological Indicators, 136*, 108718. https://doi.org/10.1016/j.ecolind.2022.108718

Vani, M., & Prasad, P. R. C. (2020). Assessment of spatio-temporal changes in land use and land cover, urban sprawl, and land surface temperature in and around Vijayawada city, India. *Environment, Development and Sustainability, 22*, 3079–3095. https://doi.org/10.1007/s10668-019-00335-2

Weerakoon, P. (2017). GIS integrated spatio-temporal urban growth modelling: Colombo urban fringe, Sri Lanka. *Journal of Geographic Information System, 09*(03), 372–389. https://doi.org/10.4236/jgis.2017.93023

Yang, M., Gong, J., Zhao, C., Zeng, Q., & Wang, Y. (2021). Landscape pattern evolution processes and the driving forces in the wetlands of lake Baiyangdian. *International Journal of Environmental Research and Public Health, 18*(9), 4403. https://doi.org/10.3390/su13179747

Yulianto, F., Fitriana, H. L., & Sukowati, K. A. D. (2020). Integration of remote sensing, GIS, and Shannon's entropy approach to conduct trend analysis of the dynamics change in urban/built-up areas in the Upper Citarum River Basin, West Java, Indonesia. *Modeling Earth Systems and Environment, 6*, 383–395. https://doi.org/10.1007/s40808-019-00686-9